Systems & Control Transactions

Original Research Article
Peer Reviewed Conference Proceeding
ESCAPE 36 - European Symposium on Computer Aided Process Engineering
Sheffield, UK. 21-24 June 2026

PSE PRESS

Comparison of Various Hydrogen Flux Trajectories in a Catalytic Membrane Reactor Operating Dehydrogenation of Ethylbenzene to Styrene

Nabeel S. Abo-Ghander[ab]*

[a] Department of Chemical Engineering, King Fahd University of Petroleum & Minerals, Dhahran 31261, Saudi Arabia.
[b] Interdisciplinary Center for Refining & Advanced Chemicals, King Fahd University of Petroleum & Minerals, Dhahran 31261, Saudi Arabia.
* Corresponding Author: naboghander@gmail.com.

ABSTRACT

Styrene is mainly produced by dehydrogenating ethylbenzene over an iron oxide-based catalyst. The reaction is endothermic and thermodynamically limited when operated in conventional catalytic fixed-bed reactors. This makes the styrene production process a conversion-selectivity trade-off, where different objectives must be compromised. In this work, a one-dimensional reactor model accounting for changes in molar flowrate, temperature, and pressure is used to predict the performance of a membrane reactor. Three main hydrogen flux profiles were assumed along the reactor axial direction: constant, linearly increasing, and linearly decreasing. It is found that the styrene yield and selectivity in a membrane reactor operated with a linearly decreasing hydrogen flux profile are higher than those with constant or linearly increasing hydrogen flux profiles in both isothermal and nonisothermal cases. It is also observed that the styrene yield and selectivity of the membrane reactor operated with a linearly decreasing hydrogen flux can be enhanced by improving the membrane's average hydrogen permeability. The influence of nonlinearity in the hydrogen flux equation is marginal and observed mainly at the reactor inlet. The improvement is due to enhanced hydrogen permeation, which is observed to be better for the linearly decreasing hydrogen profile than for the constant, linearly increasing hydrogen flux profile. When a permeation section is included in the reactor at the point where maximum hydrogen production is observed, the styrene yield is better than that of the completely permeated catalytic reactor.

Keywords: Reaction Engineering, Modelling and Simulations, Optimization, Hydrogen, Membranes, Hydrogen Flux

INTRODUCTION

Styrene is a crucial component for manufacturing high-performance polymers. It is mainly produced via the dehydrogenation reaction of ethylbenzene catalyzed by iron-oxide based catalyst. The reaction is endothermic and thermodynamically limited when operated in conventional fixed-bed reactors. This turns the process of styrene production into a conversion-selectivity problem where different objectives must be compromised.

Several researchers studied the kinetics of ethylbenzene dehydrogenation and its interactions with other chemicals. For instance, the influence of the presence of CO_2 in the reactor catalyzed by Fe_2O_3 supported on Al_2O_3 was addressed by Mimura and Saito, while the impact of the presence of steam in the reactor when ethylbenzene is dehydrogenated was studied by Zhu et al. via dynamic experiments in the presence of a potassium-promoted iron oxide-based catalyst [1, 2]. Rossetti et al. studied the causes of the deactivation of a commercial catalyst used for the dehydrogenation of ethylbenzene to styrene [3]. Lee and Froment studied the kinetics of the dehydrogenation of ethylbenzene to styrene catalyzed by a commercial iron oxide catalyst in a fundamental way, whereas Hossain M et al. studied the kinetics on a mesoporous alumina-supported iron catalyst [4, 5].

To improve styrene yield and selectivity, various reactor configurations have been proposed in the literature.

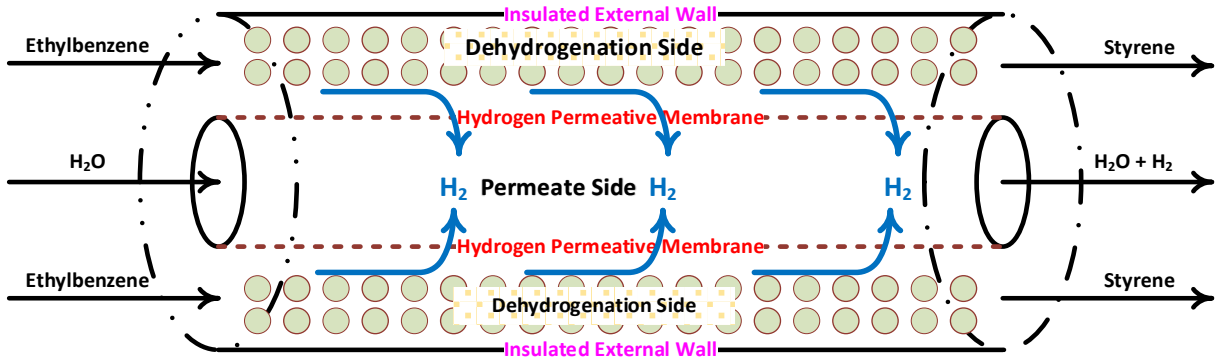

Figure 1: Cocurrent configuration of the catalytic fixed bed membrane reactor operating dehydrogenation of ethylbenzene.

For example, catalytic membrane reactors were used for the dehydrogenation of ethylbenzene to styrene, with the reaction integrated with either a sweep gas on the permeate side or with another hydrogenation reaction, such as the hydrogenation of nitrobenzene to aniline [6, 7]. Both 1D and 2D reactor mathematical models were used to describe and optimize the performance of the newly configured membrane reactors [8]. In catalytic membrane reactors, it is observed that styrene yield and selectivity were significantly improved compared to conventional fixed-bed reactors.

The performance of membrane reactors that enhance the selectivity and yield of a desired species is influenced by several parameters, among them the hydrogen permeation policy. So far, the hydrogen flux profile in membrane reactors has been estimated using Sievert's law, in which the driving force is the difference in hydrogen partial pressures between the reaction and permeate sides. The assessment of the various hydrogen permeation profiles and their impacts on reactor performance has not yet been addressed in the literature. The concept of nonuniform distribution has been already implemented in problems related to the catalyst activity within catalyst pellets and heat exchange in nonadiabatic catalytic reactors. Consequently, the main goal of this manuscript is to address the variation in hydrogen flux along the axial direction of a membrane reactor used to dehydrogenate ethylbenzene to styrene and to assess reactor performance. This will surely help reduce membrane reactor construction costs, as these costs are directly related to hydrogen permeability. Additionally, this study shed light on the problem of optimal hydrogen policy leading to the construction of optimally efficient catalytic membrane reactors.

KINETICS AND REACTION RATE LAWS

The reaction network of ethylbenzene dehydrogenation on a commercial iron oxide catalyst is composed of the following set of stoichiometric equations:

$$C_6H_5C_2H_5 \Leftrightarrow C_6H_5C_2H_3 + H_2 \quad [1]$$

$$C_6H_5C_2H_5 \rightarrow C_6H_6 + C_2H_4 \quad [2]$$

$$C_6H_5C_2H_5 + H_2 \rightarrow C_6H_5CH_3 + CH_4 \quad [3]$$

$$C_6H_5C_2H_3 + 2H_2 \rightarrow C_6H_5CH_3 + CH_4 \quad [4]$$

Two types of chemical reactions occur within the reactor: thermal and catalytic reactions, and neither can be neglected. The thermal reactions, following a radical mechanism, happen in the reactor free zone and are described by reactions [1], [2], and [3]. On the other hand, the catalytic reactions are described by reactions [1], [2], [3], and [4], which take place at the catalyst surface. The kinetic laws of thermal reactions based on molecular mechanisms and catalytic reactions based on intrinsic Hougen-Watson kinetic models are given by Lee and Froment [4].

REACTOR CONFIGURATION

The schematic diagram of the cocurrent configuration of a catalytic membrane reactor is depicted in Figure 1. The reactor is assumed to have a concentric configuration with an outer and an inner side. The outer side of the reactor is packed with a commercial iron oxide catalyst, catalyzing the dehydrogenation reaction of ethylbenzene to styrene. The reaction network is complex, leading to net endothermicity in conventional fixed-bed reactors. Benzene, toluene, and ethylene are produced as byproducts within the reactor. In conventional fixed bed reactors, hydrogen production and net endothermicity limit ethylbenzene conversion, styrene yield, and selectivity.

The external wall on the inner side of the reactor is fabricated to be hydrogen-permeable. It allows hydrogen produced on the dehydrogenation side to infiltrate to the permeate side, where pure steam is used to purge out the diffused hydrogen. Additionally, the permeate side may be used for in-situ heat exchange with the reaction side,

assisting in shifting the reaction's thermodynamic limitation. In-situ hydrogen permeation from the reaction side to the permeate side can significantly enhance the conversion and yield of ethylbenzene and styrene compared to conventional catalytic fixed-bed reactors. The external wall of the reactor on the reaction side is assumed to be perfectly insulated, preventing significant heat transfer between the reactor and its surroundings.

REACTOR MATHEMATICAL MODELLING

The mathematical model governing the performance of the catalytic membrane reactor is deduced considering the following assumptions:

1. Steady state operation
2. Ideal gas behavior on both sides of the reactor.
3. Ideal plug flow behavior.
4. Pseudo-homogeneous reactor model, i.e., neglect the transport effect between the reacting fluid and the catalyst pellets.
5. Neglecting the effect of catalyst deactivation.
6. A highly selective membrane reactor allowing only hydrogen to penetrate to the permeate side.
7. Adiabatic external wall of the membrane reactor
8. Pressure drop within the reaction side is correlated using Ergun's equation.

The reactor model equations on the reaction side of the catalytic membrane reactor may be mathematically presented as follows:

Mole balance equation on the reaction side:

$$\frac{dn_i}{dz} = \sum_{j=1}^{3} \upsilon_{ij}\, r_j^t A_c \varepsilon + \sum_{j=1}^{4} \upsilon_{ij}\, r_j^t \rho_s A_c (1-\varepsilon) - 2\pi R_3 \omega_i J_i(z) \quad [5]$$

Energy balance equation on the reaction side:

$$\frac{dT}{dz} = \frac{\begin{bmatrix} \sum_{j=1}^{3} \upsilon_{ij} r_j^t A_c \varepsilon [-\Delta H(T)]_j^t \\ + \sum_{j=1}^{4} \upsilon_{ij} r_j^t \rho_s A_c (1-\varepsilon) [-\Delta H(T)]_j \\ - \sum_{i=1}^{n} 2\pi R_3 \omega_i J_i(z) \int_{T'}^{T} C_{pi} dT + 2\pi R_3 U(T'-T) \end{bmatrix}}{\sum_{i=1}^{n} n_i C_{pi}} \quad [6]$$

Ergun's equation on the reaction side:

$$\frac{dP}{dz} = -\frac{G}{\rho g_c D_p}\left(\frac{1-\varepsilon}{\varepsilon^3}\right)\left[\frac{(1-\varepsilon)\mu}{D_p} 1.75G\right] \quad [7]$$

On the permeate side, the model equations may be stated as follows:

Mole balance equation on the permeate side:

$$\frac{dn_i'}{dz} = 2\pi R_3 \omega_i J_i(z) \quad [8]$$

Energy balance equation on the permeate side:

$$\frac{dT'}{dz} = \frac{\sum_{i=1}^{n} 2\pi R_3 \omega_i J_i(z) \int_{T'}^{T} C_{pi} dT - 2\pi R_3 U(T'-T)}{\sum_{i=1}^{n} n_i' C_{pi}'} \quad [9]$$

The boundary condition for the cocurrent flow configuration on both sides of the membrane reactor is defined at the reactor inlet as follows:

At $z = 0$:

$$n_i = n_{i0} \quad T = T_0 \quad P = P_0 \quad n_i' = n_{i0}' \quad T' = T_0' \quad [10]$$

In Eqs. [5], [6], [8], and [9], the Greek letter "ω_i" was introduced to make the derived model usable for both a conventional fixed bed reactor and a membrane catalytic reactor. If "$\omega_i = 0$" the model predicts the performance of the conventional fixed bed reactor, while "$\omega_i = 1$" the performance of the catalytic membrane reactor is predicted.

The set of reactor model equations forms an initial-value problem (IVP) that must be solved numerically using a suitable numerical method. In this work, a finite element orthogonal collocation technique is implemented using a predefined number of points per interval, thereby transforming the system of differential equations into a set of nonlinear algebraic equations. The set of algebraic equations has been solved using the "fsolve" MATLAB subroutine.

REACTOR PERFORMANCE MEASURE

The reactor performance indexes considered in this study are ethylbenzene conversion, styrene yield, and styrene selectivity. They are all estimated using the following equations:

$$x_{EB} = \frac{n_{EB,0} - n_{EB}}{n_{EB,0}} \quad [11]$$

$$Y_{ST} = \frac{n_{ST} - n_{ST,0}}{n_{EB,0}} \quad [12]$$

$$S_{ST} = \frac{n_{ST} - n_{ST,0}}{n_{EB,0} - n_{EB}} \quad [13]$$

These performance measures are generally conflicting; maximizing one leads to minimizing the others. As a result, multi-objective optimization problems that combine these measures might be considered at later stages of this study.

PROBLEM MATHEMATICAL FORMULATION

This study aims to investigate and assess the impact of implementing different hydrogen-permeation policies on the performance of a membrane reactor used for the dehydrogenation of ethylbenzene to styrene. The molar flux profile in the reactor model equation is given by the term $J_i(z)$ and it is defined only for hydrogen. The following mathematical model predicting the molar hydrogen flux as a function of axial distance is implemented in the reactor model equations:

$$J_{H_2}(z) = az^{\alpha} + b \quad [14]$$

The parameters "a" and "b" in the above equation

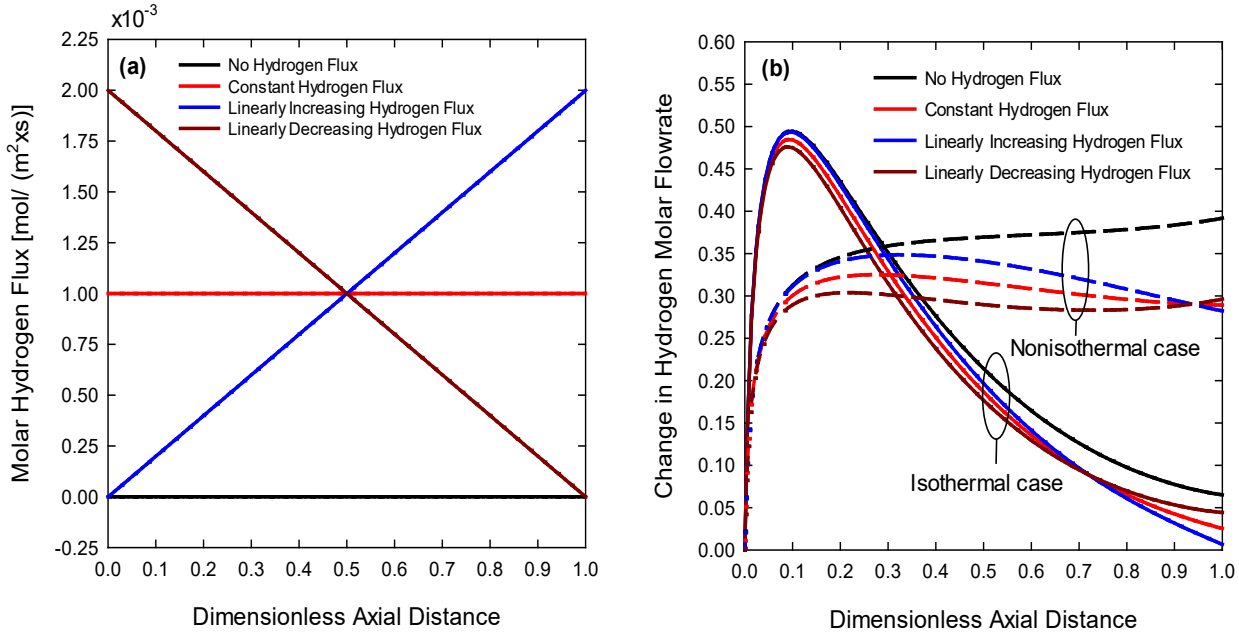

Figure 2: (a) hydrogen flux profiles implemented in the cocurrent configuration of the membrane reactor with an average permeability of 1.0×10^{-3} mol/(m²×s). (b) change in hydrogen molar flowrates for both isothermal and nonisothermal cases.

have the units of mol/($m^{\alpha+2}$×s) and mol/(m²×s), respectively. Adjusting "α" in the above model provides a variety of linear and nonlinear distributions, i.e., α=0 is constant, α=1 is linear, and α≠1 is nonlinear. Three types of monotonic hydrogen fluxes may be defined: constant hydrogen flux, an increasing molar flux set to zero at the reactor feeding point, and a decreasing molar flux set to zero at the reactor exit. Consequently, the hydrogen molar flux is given for α≠1 as a function of the dimensionless distance $\zeta = \frac{z}{L}$ as follows:

Constant hydrogen flux:

$$J_{H_2}(z) = J_{ave} = \bar{J} \qquad [15]$$

Monotonically increasing hydrogen flux for $0 \le \zeta \le 1$ and $\zeta_1 < \zeta_2$:

$$J_{H_2}(\zeta) = \frac{(1+\alpha)(\zeta_2-\zeta_1)\bar{J}(\zeta^\alpha-\zeta_1^\alpha)}{\zeta_2(\zeta_2^\alpha-\zeta_1^\alpha)-\alpha\zeta_1^\alpha(\zeta_2-\zeta_1)} \qquad [16]$$

Monotonically decreasing hydrogen flux for $0 \le \zeta \le 1$ and $\zeta_1 < \zeta_2$:

$$J_{H_2}(\zeta) = \frac{(1+\alpha)(\zeta_2-\zeta_1)\bar{J}(\zeta^\alpha-\zeta_2^\alpha)}{\zeta_1(\zeta_2^\alpha-\zeta_1^\alpha)-\alpha\zeta_2^\alpha(\zeta_2-\zeta_1)} \qquad [17]$$

In the above molar flux models, the average membrane permeability in the above equations is defined as:

$$J_{ave} = \bar{J} = \frac{1}{L}\int_0^L J_{H_2}(z)dz = \int_0^1 J_{H_2}(\zeta)d\zeta \qquad [18]$$

In this study, the influence of average membrane permeability, nonlinearity, and hydrogen flux on the performance of the catalytic membrane reactor is examined primarily under isothermal conditions. The behavior of the membrane reactor under adiabatic, nonisothermal operating conditions is also presented to extend the conclusions. The focus is mainly on the isothermal condition, as establishing net endothermicity in the nonisothermal reactor will influence reaction kinetics and equilibrium conversion. Hence, the assessment of reactor performance will also be affected by temperature variations.

REACTOR OPERATING CONDITIONS

The geometric parameters and operating conditions used to simulate the performance of the catalytic membrane reactor are summarized in Table 1.

These parameters were kept constant while varying the trajectories of the molar hydrogen flux along the reactor axial distance and accounting for changes in related parameters, such as membrane permeability and the nonlinearity of the hydrogen flux profiles.

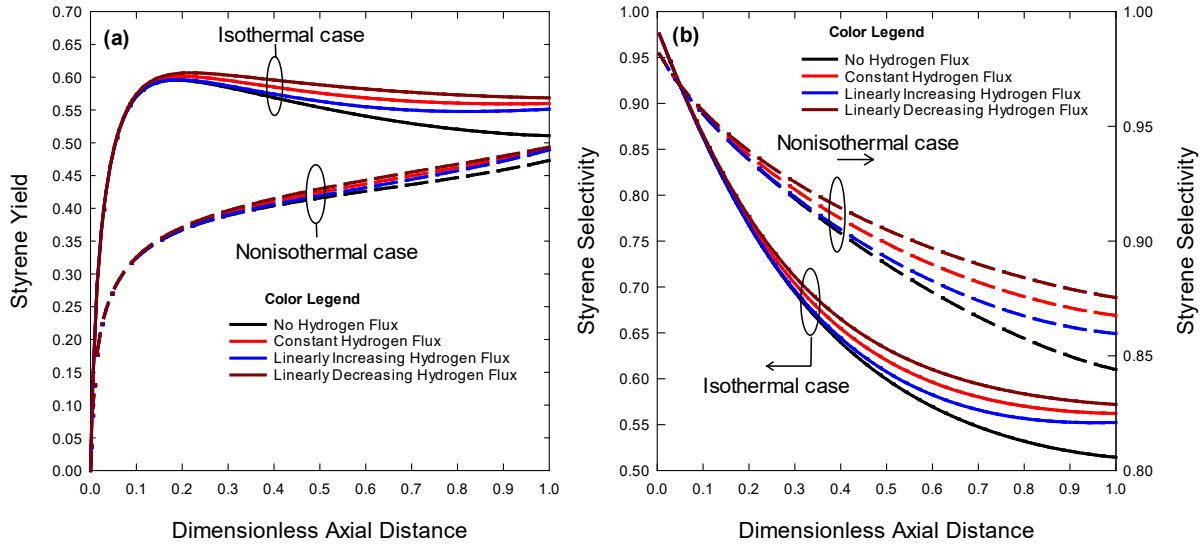

Figure 3: (a) styrene yield along the dimensionless axial distance of the reactor for both isothermal and nonisothermal cases. (b) selectivity to styrene along the dimensionless axial distance of the reactor for both isothermal and nonisothermal cases.

Table 1: List of operating and design parameters of the catalytic membrane reactor

Parameter	Value	Unit
Design Parameters		
Reactor length	0.22	m
Diameter of the permeate side	0.080	m
Equivalent diameter of the reaction side	0.055	m
Voidage	0.4312	--
Diameter of the catalyst particle	0.020	m
Operating Parameters		
Reaction side:		
Total input molar flowrate	1.0×10^{-2}	mol/s
Ethylbenzene mole fraction	0.08321	--
Styrene mole fraction	8.3612×10^{-4}	--
Benzene mole fraction	3.4485×10^{-5}	--
Toluene mole fraction	5.8472×10^{-4}	--
Steam mole fraction	0.9153	--
Feed temperature	886	K
Feed pressure	2.5	bar
Permeate side:		
Steam molar flowrate	0.01	mol/s
Feed temperature	1000	K
Feed pressure	1.0	bar

RESULTS AND DISCUSSION

In this study, the three basic molar hydrogen flux profiles considered, i.e., constant, linearly increasing, and linearly decreasing profiles, are shown in Figure 2a. For the constant molar hydrogen flux profile, the average molar hydrogen flux is maintained along the reactor, unlike the linearly increasing hydrogen flux profile, where the maximum permeability is observed at the reactor exit, or the linearly decreasing hydrogen flux profile, where the maximum permeability is observed at the reactor inlet.

In Figure 2b, the changes in the hydrogen molar flowrate defined as the difference in hydrogen molar flowrate to the ethylbenzene fed, are plotted along the axial distance of the reactor for the conventional fixed reactor, and the catalytic membrane reactor operated isothermally and nonisothermally. The maximum reduction in hydrogen on the reaction side of the membrane reactor occurs with a linearly decreasing hydrogen flux, followed by a linearly increasing hydrogen flux, and then a constant hydrogen flux profile. This observation is consistent whether the membrane reactor is operated isothermally or nonisothermally.

The influence of the application of the linear molar hydrogen flux profiles on the styrene yield and selectivity to styrene is depicted in Figure 3. In Figure 3a, the styrene yield is plotted as a function of the reactor axial distance for both the conventional catalytic fixed reactor and the catalytic membrane reactor, operated with three

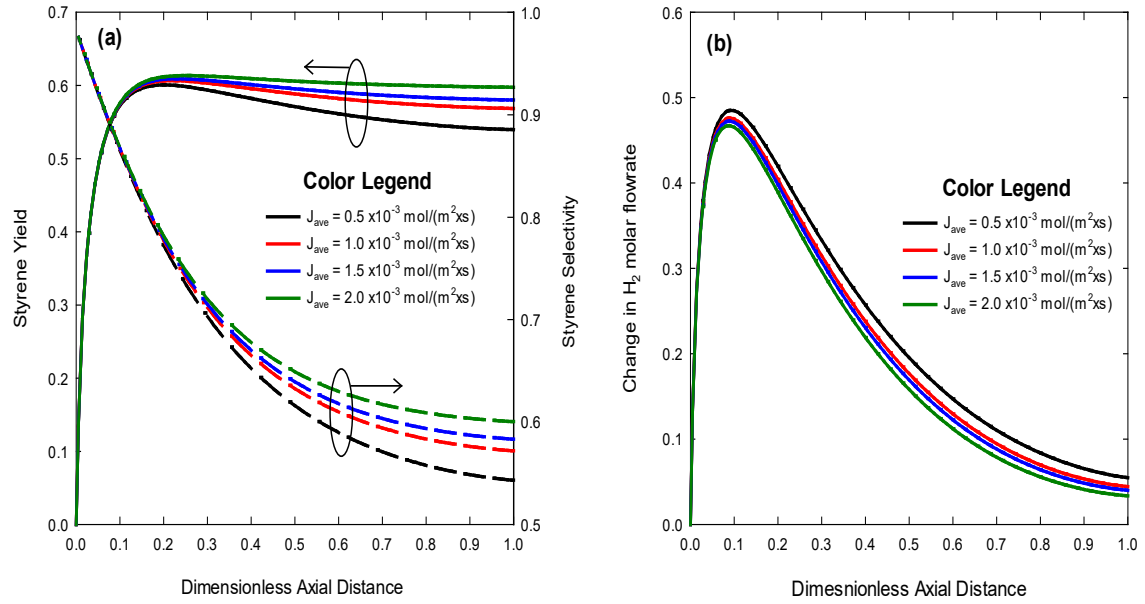

Figure 4: Influence of the average permeability of hydrogen on (a) styrene yield and selectivity to styrene and (b) change in hydrogen molar flowrate along the dimensionless axial distance of the reactor for the linearly decreasing hydrogen flux case.

different molar hydrogen flux profiles. It is found that the catalytic membrane reactor outperforms the conventional fixed-bed reactor, and the membrane reactor with a linearly decreasing hydrogen molar flux performs better than those with linearly increasing or constant hydrogen flux profiles.

This is because hydrogen permeation is significantly enhanced when linearly decreasing hydrogen flux profiles are used. The styrene selectivity along the reactor axial direction is plotted in Figure 3b. It is also observed that the performance of the catalytic membrane reactor with a linearly decreasing hydrogen molar profile exceeds that of conventional catalytic fixed reactors and of catalytic membrane reactors with linearly increasing or constant hydrogen flux profiles.

The effect of changing the average membrane permeability is assessed for a linearly decreasing hydrogen flux profile in Figure 4, where styrene yield, styrene selectivity, and change in hydrogen molar flowrate are plotted along the reactor axial distance. The values of 0.5×10^{-3}, 1.0×10^{-3}, 1.5×10^{-3}, and 2.0×10^{-3} mol/(m^2×s) were chosen to evaluate the performance of the membrane reactor under a linearly decreasing molar flux profile.

In Figure 4a, both the styrene yield and the styrene selectivity are plotted as a function of membrane reactor length for all four values of membrane permeability. It is found that as permeability increases, both the overall styrene yield and the styrene selectivity increase from ~0.53 to ~0.60. This refers to the permeation of hydrogen whose molar flow rate change is plotted along the axial distance of the membrane reactor in Figure 4b. It is shown that as membrane permeability increases, the hydrogen flowrate decreases on the reaction side, thereby enhancing both the styrene yield and selectivity to styrene

The effect of nonlinearity in the creasing flux equation is depicted in Figure 5. For α=0.3, α=1.0, and α=2.0, three nonlinearly decreasing hydrogen flux profiles are plotted along the reactor axial distance in Figure 5a. It is observed that increasing the value of "α" increases permeability at the reactor inlet, and it is higher for α=0.3 than for α=1.0 or α=2.0.

In Figure 5b, both the styrene yield and the change in hydrogen molar flowrate are plotted as a function of the reactor dimensionless distance for α=0.3, α=1.0, and α=2.0. It is found that as the value of "α" decreases, the styrene yield enhances at the reactor inlet, where the hydrogen flux is significant due to the decrease in the hydrogen molar flowrate. This suggests that when ethylbenzene is dehydrogenated in a catalytic membrane reactor, the maximum permeation should occur at the reactor inlet, where the hydrogen molar flow rate is high.

The impact of introducing a permeation section in an existing fixed bed reactor is also assessed in this study. Linearly decreasing hydrogen flux profiles with an average hydrogen molar flow rate of 3.0×10^{-3} mol/(m^2×s) are sketched along the reactor dimensionless axial distance

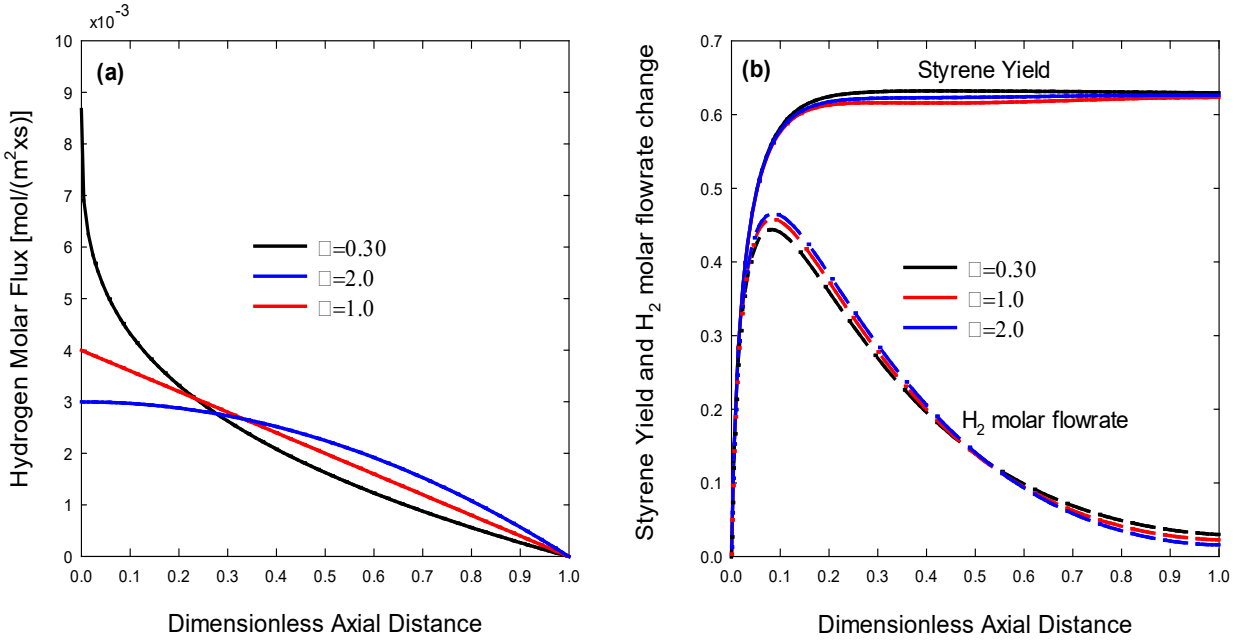

Figure 5: Influence of the nonlinearity in the hydrogen permeation model on (a) hydrogen flux, (b) styrene yield, and change in hydrogen molar flowrate along the dimensionless axial distance of the reactor for the linearly decreasing hydrogen flux case.

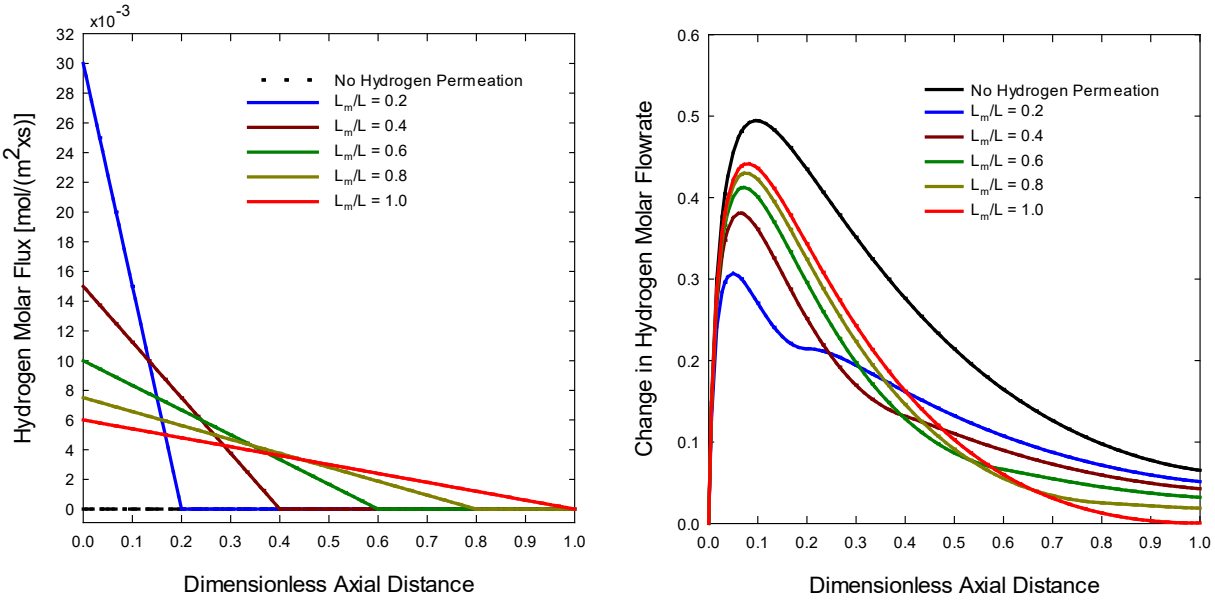

Figure 6: (a) decreasing hydrogen molar flux profiles applied at different fractions of the reactor length, (b) the corresponding change in hydrogen molar flowrate along the reactor axial distance.

in Figure 6a.

As the permeation fraction varies between 0.0 (non-permeable reactor) and 1.0 (Fully permeable reactor), a significant reduction in the hydrogen molar flow rate is observed, as shown in Figure 6b, compared to the conventional fixed bed reactor. The hydrogen molar flow rate increases at the beginning of the reactor due to the dehydrogenation of ethylbenzene, then falls after reaching a maximum at which the rate of hydrogen production is balanced by the rate of hydrogen permeation.

This shows that there is an optimal length when maximizing styrene production is the goal. The optimal

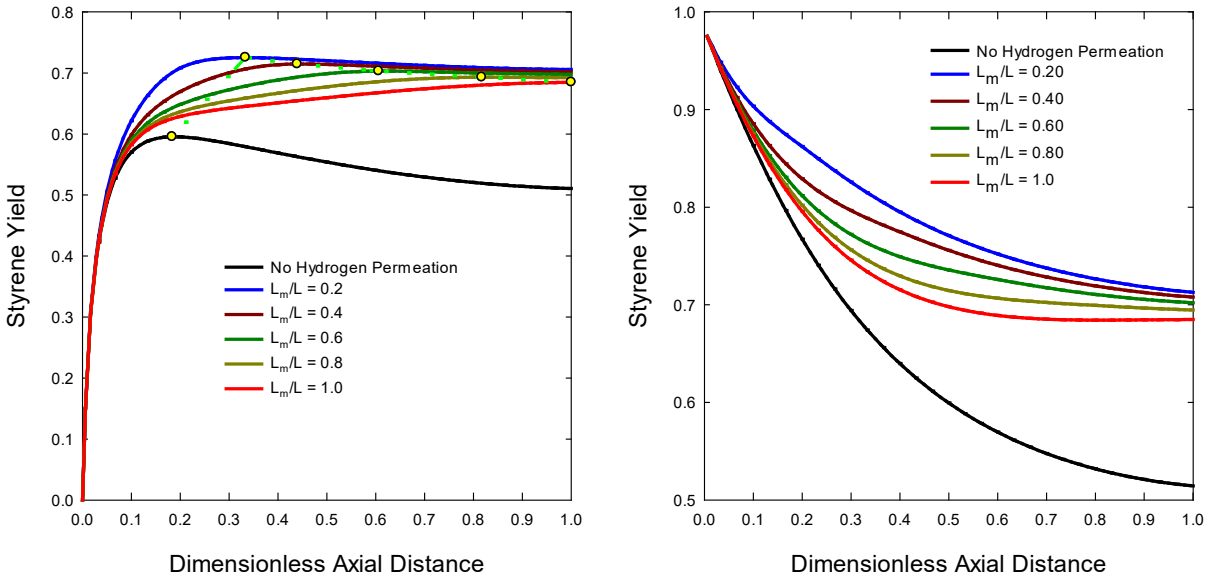

Figure 7: (a) styrene yield and (b) tyrene selectivity along the reactor axial distance for different fractions of the permeation section.

reactor fractional length is shown in Figure 7a by the light green curve, and a summary of the computed optimal reactor fractional length is given in Table 2. Based on the results summarized in Table 2, increasing the fraction of the permeation section within the reactor while maintaining the same average hydrogen permeation rate shifts the optimal reactor length to the right, improving yield. In general, the presence of a nonpermeating section in the reactor is detrimental, as it causes styrene to react with residual hydrogen to produce toluene. This unpleasant effect becomes more pronounced as the permeation section within the reactor is shortened. However, when a permeation section is placed around the point of maximum hydrogen production, the styrene yield in the reactor improves.

For instance, when the permeation section is placed within the first 20% of the reactor length, the predicted styrene yield is 0.73, the highest among all the trials considered. As far as styrene selectivity is concerned, it improves as the fraction of the reactor's permeation section increases.

Table 2: Summary of the optimal reactor length required to maximize styrene yield

Applied fraction of the permeation section	Optimal Reactor fractional length	Maximum styrene yield	Comment
0	0.18	0.60	No Permeation
0.20	0.33	0.73	--
0.40	0.44	0.71	--
0.60	0.61	0.70	--
0.80	0.82	0.69	--
1.0	1.00	0.68	Fully Permeated reactor

CONCLUSION AND RECOMMENDATIONS

The computational analysis of the impact of applying theoretical molar hydrogen profiles on the performance of a catalytic membrane reactor used for the dehydrogenation of ethylbenzene to styrene has been conducted using a one-dimensional reactor model that accounts for changes in molar flowrate, temperature, and

pressure on both the reaction and permeate sides. Three main molar hydrogen profiles are tested, namely constant, linearly increasing, and linearly decreasing profiles, and the performance of the catalytic membrane reactor is assessed via styrene yield and selectivity to styrene. It is found that the reactor should be designed to achieve a maximum hydrogen permeation rate at the inlet section, thereby enhancing styrene yield and selectivity. This can be achieved by applying linearly decreasing molar hydrogen profiles, which are more attractive than constant or linearly increasing hydrogen permeation profiles. Yet, with linearly decreasing hydrogen permeation profiles, the reactor's performance can be further enhanced by adopting a shell-and-tube configuration, which increases the available surface area for hydrogen permeation. Hydrogen membranes with linearly decreasing hydrogen profiles can be fabricated by correlating the palladium distribution with the hydrogen permeation rate. The steam feeding strategy on the permeate side might also be used to adjust the permeation rate of existing membranes to match the linear hydrogen flux observed in this work. The application of these results can significantly promote the use of hydrogen membranes with varying permeabilities in chemical reactors, thereby reducing construction costs. In addition, the results here shed light on the optimal hydrogen flux trajectory required to maximize the styrene yield and selectivity. Adding a permeation section around the point where maximum hydrogen is observed is preferable and yields higher conversion than a completely permeable reactor.

NOMENCLATURE:

A_c: reactor cross-sectional area, [m^2].
D_p: diameter of the catalyst pellet, [m].
G: mass velocity of the reacting mixture, [Kg/(m^2×s)].
$J_i(z)$: molar flux of species i along the axial distance of the reactor, [mol/(m^2×s)].
$J_{ave} or \bar{J}$: average molar flux of species i, [mol/(m^2×s)].
n_i: molar flowrate of species i in the reaction side of the reactor, [mol/s].
L: reactor length, [m].
P: Pressure in the reaction side of the reactor, [K].
r_j^c: catalytic reaction rate of j reaction, [mol/(Kg×s)].
r_j^t: thermal reaction rate of j reaction, [mol/(m^3×s)].
T: Temperature on the reaction side of the reactor, [K].
T': Temperature on the permeate side of the reactor, [K].
U: overall heat transfer coefficient, [J/(m^2×K×s)].
z: reactor axial distance, [m].
ζ: dimensionless reactor axial distance, [-].
μ: Viscosity of the reacting mixture, [Pa×s].
υ_{ij}: stoichiometric no. of species i in j reaction, [-].
ρ: density of the reacting mixture, [kg/m^3].
ρ_s: density of the catalyst particles, [kg/m^3].
ε: bed void fraction, [-].
ζ_1: the start of the membrane section, [-].
ζ_2: the end of the membrane section, [-].

ACKNOWLEDGEMENTS

The author would like to thank King Fahd University of Petroleum & Minerals (KFUPM) and the Interdisciplinary Center for Refining & Advanced Chemicals for the financial support.

DEDICATION

Dedicated to the soul of my great mentor, PhD advisor, and scholar, Prof. John R. Grace, who taught me scientific ethics, manners, and appreciation.

REFERENCES

1. Mimura N, Saito M. Dehydrogenation of ethylbenzene to styrene over fe2o3/al2o3 catalysts in the presence of carbon dioxide. Catalysis Today 55:173-178 (2000). https://doi.org/10.1016/s0920-5861(99)00236-9
2. Zhu XM, Schön M, Bartmann U, van Veen AC, Muhler M. The dehydrogenation of ethylbenzene to styrene over a potassium-promoted iron oxide-based catalyst: a transient kinetic study. Applied Catalysis A: General 266:99-108 (2004). https://doi.org/10.1016/j.apcata.2004.02.002
3. Rossetti I, Bencini E, Trentini L, Forni L. Study of the deactivation of a commercial catalyst for ethylbenzene dehydrogenation to styrene. Applied Catalysis A: General 292:118-123 (2005). https://doi.org/10.1016/j.apcata.2005.05.046
4. Jae Lee W, Froment GF. Ethylbenzene dehydrogenation into styrene: kinetic modeling and reactor simulation. Ind. Eng. Chem. Res. 47:9183-9194 (2008). https://doi.org/10.1021/ie071098u
5. Hossain MM, Atanda L, Al-Yassir N, Al-Khattaf S. Kinetics modeling of ethylbenzene dehydrogenation to styrene over a mesoporous alumina supported iron catalyst. Chemical Engineering Journal 207-208:308-321 (2012). https://doi.org/10.1016/j.cej.2012.06.108
6. Hermann C, Quicker P, Dittmeyer R. Mathematical simulation of catalytic dehydrogenation of ethylbenzene to styrene in a composite palladium membrane reactor. Journal of Membrane Science 136:161-172 (1997). https://doi.org/10.1016/s0376-7388(97)81990-4
7. Abo-Ghander NS, Grace JR, Elnashaie SSEH, Lim CJ. Modeling of a novel membrane reactor to integrate dehydrogenation of ethylbenzene to styrene with hydrogenation of nitrobenzene to

aniline. Chemical Engineering Science 63:1817-1826 (2008). https://doi.org/10.1016/j.ces.2007.12.007

8. Abo-Ghander NS, Logist F, Grace JR, Van Impe JFM, Elnashaie SSEH, Lim CJ. Optimal design of an autothermal membrane reactor coupling the dehydrogenation of ethylbenzene to styrene with the hydrogenation of nitrobenzene to aniline. Chemical Engineering Science 65:3113-3127 (2010). https://doi.org/10.1016/j.ces.2010.02.007